A click-by-click strategy ...

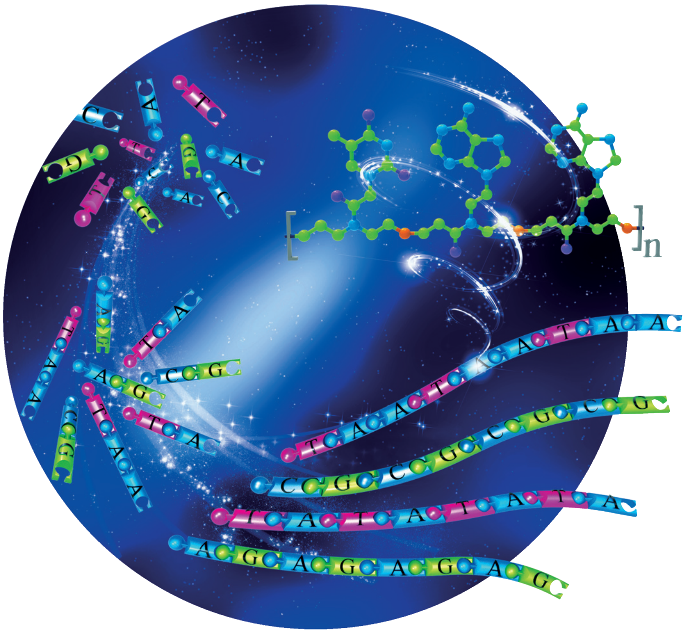

... that is based on orthogonal thiol-X click reactions is used for the synthesis of nucleobase-functionalized sequence-controlled periodic polymer structures in a simple and efficient process. As demonstrated by C. N. Bowman and co-workers in their Communication on page 14462 ff., this method enables the formation of highly functional materials, including a new class of synthetic oligonucleotides, in a robust, scalable manner.

NMR Spectroscopy

C. R. Bowers, H. E. Hagelin-Weaver et al. describe in their Communication on page 14270 ff. how intense NMR signals are induced by incorporating para-H_2 into propene and propane over octahedron-, cube-, or rod-shaped ceria nanocrystals.

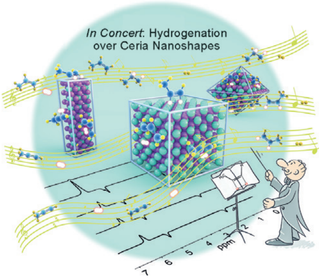

Vapor Sensors

In their Communication on page 14317 ff., M. Pumera and co-workers develop a vapor sensor based on layered black phosphorus for selective methanol detection by electrochemical impedance spectroscopy.

Paraffin Separation

Metal–organic frameworks (MOFs) with the ideal pore-aperture size for the total exclusion of branched paraffins from normal paraffins are reported by M. Eddaoudi and co-workers in their Communication on page 14353 ff.

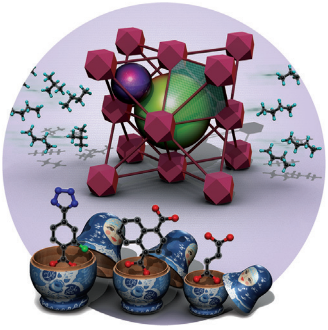

How to contact us:

Editorial Office:
E-mail: angewandte@wiley-vch.de
Fax: (+49) 6201–606-331
Telephone: (+49) 6201–606-315

Reprints, E-Prints, Posters, Calendars:
Carmen Leitner
E-mail: chem-reprints@wiley-vch.de
Fax: (+49) 6201–606-331
Telephone: (+49) 6201–606-327

Copyright Permission:
Bettina Loycke
E-mail: rights-and-licences@wiley-vch.de
Fax: (+49) 6201–606-332
Telephone: (+49) 6201–606-280

Online Open:
Margitta Schmitt
E-mail: angewandte@wiley-vch.de
Fax: (+49) 6201–606-331
Telephone: (+49) 6201–606-315

Subscriptions:
www.wileycustomerhelp.com
Fax: (+49) 6201–606-184
Telephone: 0800 1800536 (Germany only)
+44(0) 1865476721 (all other countries)

Advertising:
Marion Schulz
E-mail: mschulz@wiley-vch.de
Fax: (+49) 6201–606-550
Telephone: (+49) 6201–606-565

Courier Services:
Boschstrasse 12, 69469 Weinheim

Regular Mail:
Postfach 101161, 69451 Weinheim

Angewandte Chemie International Edition is a journal of the Gesellschaft Deutscher Chemiker (GDCh), the largest chemistry-related scientific society in continental Europe. Information on the various activities and services of the GDCh, for example, cheaper subscription to *Angewandte Chemie International Edition*, as well as applications for membership can be found at **www.gdch.de** or can be requested from GDCh, Postfach 900440, D-60444 Frankfurt am Main, Germany.

GDCh
GESELLSCHAFT DEUTSCHER CHEMIKER

Service

Spotlight on Angewandte's Sister Journals **14220 – 14223**

Author Profile

“My favorite food is eggs benedict.
My favorite song is Comfortably Numb (Pink Floyd) …”
This and more about Neil Burford can be found on page 14224.

Neil Burford **14224**

Obituaries

John T. Yates, Jr., professor at the University of Virginia, member of the US National Academy of Sciences, and pioneer of modern surface science passed away at the age of 80 on September 26, 2015. The scientific community has lost an exceptional scientist and gifted communicator, who was also heavily involved with scientific societies and academies, as well as evaluation procedures and conference organization.

John T. Yates, Jr. (1935–2015)

G. Ertl,* H.-J. Freund* **14225**

Books

Information, Entropy, Life and the Universe — Arieh Ben-Naim — *reviewed by F. Simmel** **14226**

Highlights

Organocatalysis

M. Waser,* J. Novacek ___ **14228 – 14231**

An Organocatalytic Biomimetic Strategy Paves the Way for the Asymmetric Umpolung of Imines

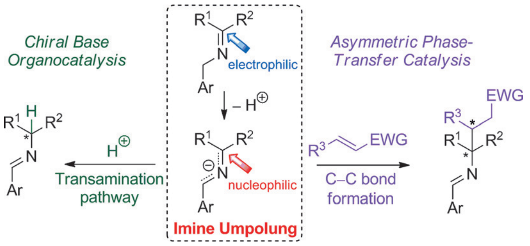

Just like Nature: A recently developed enantioselective organocatalytic biomimetic transamination provides an elegant approach towards chiral amines. In the presence of an asymmetric phase-transfer catalyst, the intermediate anionic species undergoes an asymmetric C–C bond-forming reaction in a powerful and broadly applicable asymmetric umpolung strategy.

Minireviews

Catalytic Radical Reactions

J. Streuff,* A. Gansäuer* **14232 – 14242**

Metal-Catalyzed β-Functionalization of Michael Acceptors through Reductive Radical Addition Reactions

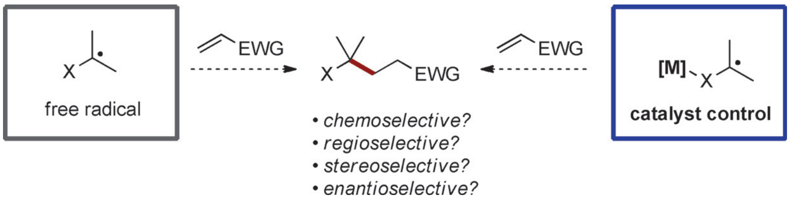

Selective radical coupling: Catalytic reductive radical additions to α,β-unsaturated compounds have gained substantial attention because of their broad applicability in organic synthesis. This Minireview discusses recent landmark achievements in the field in the context of earlier studies that provided the basis for their development.

Reviews

Molecular Magnetism

E. J. L. McInnes, G. A. Timco,
G. F. S. Whitehead,
R. E. P. Winpenny* ______ **14244 – 14269**

Heterometallic Rings: Their Physics and use as Supramolecular Building Blocks

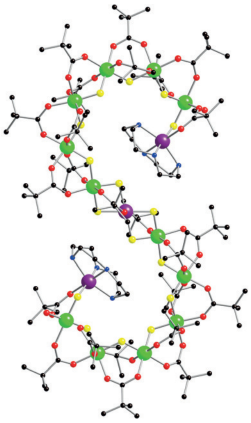

A playground for physics: Heterometallic rings featuring seven trivalent and a single divalent metal center were first reported in 2003. Since that time they have been shown to be ideal for studying the physics of anti-ferromagnetically coupled nanomagnets. They have a rich chemistry, and can be incorporated in larger structures in at least three ways, including use of the inorganic rings as part of hybrid rotaxanes.

For the USA and Canada:
ANGEWANDTE CHEMIE International Edition (ISSN 1433-7851) is published weekly by Wiley-VCH, PO Box 101161, 69451 Weinheim, Germany. US mailing agent: SPP, PO Box 437, Emigsville, PA 17318. Periodicals postage paid at Emigsville, PA. US POSTMASTER: send address changes to *Angewandte Chemie*, John Wiley & Sons Inc., C/O The Sheridan Press, PO Box 465, Hanover, PA 17331. Annual subscription price for institutions: US$ 11.738/10.206 (valid for print and electronic / print or electronic delivery); for individuals who are personal members of a national chemical society prices are available on request. Postage and handling charges included. All prices are subject to local VAT/sales tax.

NMR Spectroscopy

E. W. Zhao, H. Zheng, R. Zhou,
H. E. Hagelin-Weaver,*
C. R. Bowers* ———— 14270 – 14275

Shaped Ceria Nanocrystals Catalyze Efficient and Selective Para-Hydrogen-Enhanced Polarization

Intense NMR signals are induced by the incorporation of para-hydrogen into propene and propane through pairwise addition and replacement over octahedron-, cube-, or rod-shaped ceria nanocrystals. The synthesis of ceria nanoparticles with well-defined shapes and different surface facets was essential to gaining detailed insights into the mechanisms of these processes.

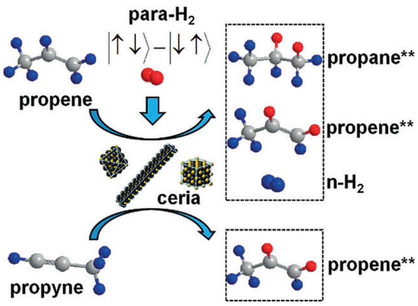

Frontispiece

Protein Engineering

Y. Guo, D.-M. Sun, F.-L. Wang, Y. He,
L. Liu,* C.-L. Tian* ———— 14276 – 14281

Diaminodiacid Bridges to Improve Folding and Tune the Bioactivity of Disulfide-Rich Peptides

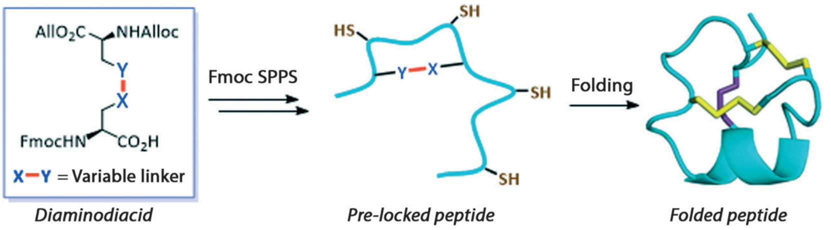

Diaminodiacid *Pre-locked peptide* *Folded peptide*

Bridging the gap: A single cystine-to-diaminodiacid replacement can enable the efficient production and optimization of disulfide-rich peptides. The practicability and advantages of this method were demonstrated through studies with the μ-conotoxin SIIIA, the hormone hepcidin, and the trypsin inhibitor EETI-II.

Hybrid Aerogels

S. Zhao, W. J. Malfait, A. Demilecamps,
Y. Zhang, S. Brunner, L. Huber, P. Tingaut,
A. Rigacci, T. Budtova,*
M. M. Koebel* ———— 14282 – 14286

Strong, Thermally Superinsulating Biopolymer–Silica Aerogel Hybrids by Cogelation of Silicic Acid with Pectin

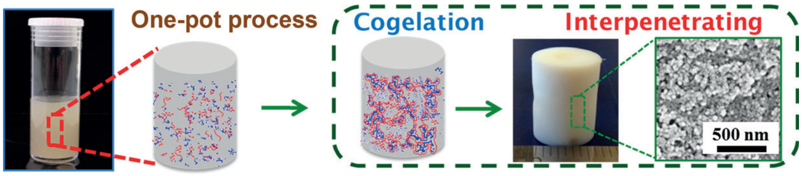

The reinforcement of silica aerogels with pectin leads to hybrid materials with superior hydrophobic, thermal, and mechanical behavior. Their structural and physical properties can be tuned by adjusting the gelation pH and pectin concentration. The structural reinforcement correlates with a change in morphology towards mechanically more favorable neck-free structures.

Inside Cover

Organometallic Emitters

R. Kumar, A. Linden,
C. Nevado* ———— 14287 – 14290

Luminescent (N^C^C) Gold(III) Complexes: Stabilized Gold(III) Fluorides

(N^C^C) Gold(III) complexes have been prepared enabling the isolation of the corresponding gold(III) fluorides in monomeric, easy-to-handle, bench-stable form by a Cl/F ligand-exchange reaction. These complexes present improved photophysical properties paving the way for the design of new late transition metal based OLEDs.

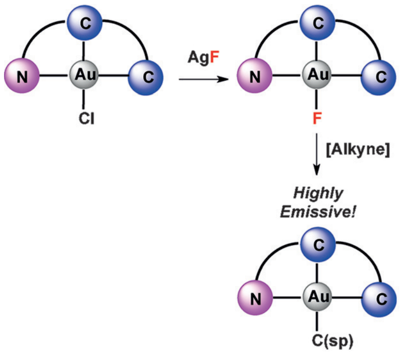

Nanobubble Assembly

Y. Wang, G. Liu,* H. Hu, T. Y. Li,
A. M. Johri, X. Li, J. Wang **14291 – 14294**

Stable Encapsulated Air Nanobubbles in Water

Fluorinated polymers were used to encapsulate air nanobubbles. The encapsulated air bubbles are echogenic and display significantly greater stability to sonication compared to commercially available microcapsules. Such features may open the door to applications in diagnostics and drug delivery.

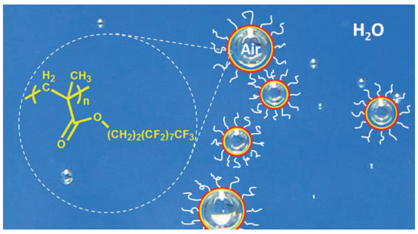

Cycloaddition

H. Wang, X. Cao, X. Chen,* W. Fang,
M. Dolg* **14295 – 14298**

Regulatory Mechanism of the Enantioselective Intramolecular Enone [2+2] Photocycloaddition Reaction Mediated by a Chiral Lewis Acid Catalyst Containing Heavy Atoms

Going for a spin: Ab initio calculations at the CASPT2//CASSCF level of theory show that the enantioselective enone [2+2] photocycloaddition (PCA) reaction is predominantly controlled by an enhanced spin–orbit coupling of the heavy atoms in the chiral Lewis acid catalyst. These mechanistic insights provide useful benchmarks for further studies of PCA reactions mediated by Lewis acids.

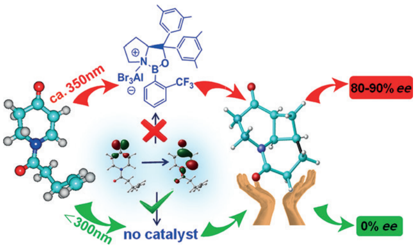

Nanocrystal Growth

D. Franke, D. K. Harris, L. Xie,
K. F. Jensen,
M. G. Bawendi* **14299 – 14303**

The Unexpected Influence of Precursor Conversion Rate in the Synthesis of III–V Quantum Dots

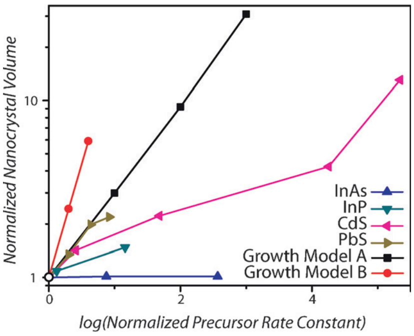

It's different: Experimental results for II–VI and IV–VI quantum dots (QDs) imply that the rate of precursor conversion during QD synthesis plays a key role for controlling QD size and size distribution. While these results agree with predictions from kinetic growth models, the current study shows that precursor chemistry and conversion rates have a much weaker influence on the growth of III–V QDs.

Single-Molecule Studies

C. Huang, S. Chen, K. Baruël Ørnsø,
D. Reber, M. Baghernejad, Y. Fu,
T. Wandlowski, S. Decurtins, W. Hong,*
K. S. Thygesen,*
S.-X. Liu* **14304 – 14307**

Controlling Electrical Conductance through a π-Conjugated Cruciform Molecule by Selective Anchoring to Gold Electrodes

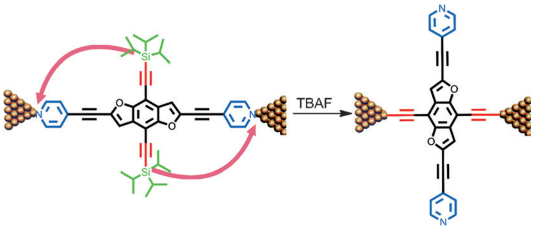

Singled out: For the first time, it has been demonstrated that two distinct charge-transport pathways, through a cruciform molecule at the single-molecule level, can be tuned by chemically controlling the anchoring sites. Upon in situ cleavage of the triisopropylsilyl group, complete conversion from the N–Au junctions into C–Au junctions is achieved with a conductance increase of more than one order of magnitude. TBAF = tetra-*n*-butylammonium fluoride.

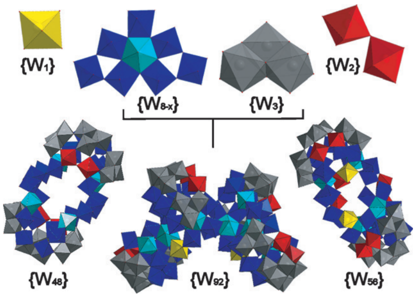

High nuclearity isopolyoxotungstates (isoPOTs) of formulae $[H_{12}W_{48}O_{164}]^{28-}$, $[H_{20}W_{56}O_{190}]^{24-}$ and $[H_{12}W_{92}O_{311}]^{58-}$ are made of unique $\{W_{21}O_{72}\}$ building units containing pentagonal $\{W(W_5)\}$, $\{W(W_4)\}$, and $\{W(W_3)\}$ motifs. The growth of these $\{W_{21}O_{72}\}$ building blocks allows for the formation of large isoPOTs with chiral features.

Isopolyoxotungstates

C. Zhan, R. S. Winter, Q. Zheng, J. Yan, J. M. Cameron, D.-L. Long,* L. Cronin* ______ **14308 – 14312**

Assembly of Tungsten-Oxide-Based Pentagonal Motifs in Solution Leads to Nanoscale $\{W_{48}\}$, $\{W_{56}\}$, and $\{W_{92}\}$ Polyoxometalate Clusters

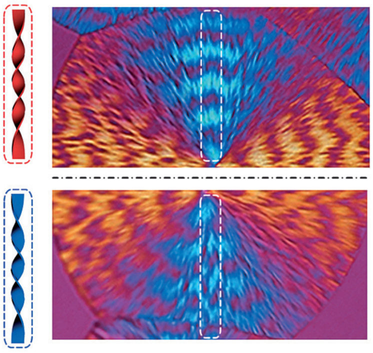

Not just a pretty pattern: The handedness of twisted lamellae in the banded spherulites of isotactic poly(2-vinylpyridine) (iP2VP) was controlled by the crystallization of iP2VP with chiral dopants (see polarized-light micrographs). Hexahydromandelic acid (HMA) induced circular dichroism in iP2VP. The mirror-image CD spectra observed with (*R*)- and (*S*)-HMA suggest homochiral evolution from conformational to hierarchical chirality in this system.

Supramolecular Chirality

T. Wen, H.-Y. Shen, H.-F. Wang, Y.-C. Mao, W.-T. Chuang, J.-C. Tsai,* R.-M. Ho* ______ **14313 – 14316**

Controlled Handedness of Twisted Lamellae in Banded Spherulites of Isotactic Poly(2-vinylpyridine) as Induced by Chiral Dopants

Methanol detection: A vapor sensor that is based on layered black phosphorus and uses electrochemical impedance spectroscopy as the detection method selectively detects methanol. The impedance phase measured at a constant frequency is used as a distinctive parameter for the quantification of the methanol concentration with a low detection limit of 28 ppm.

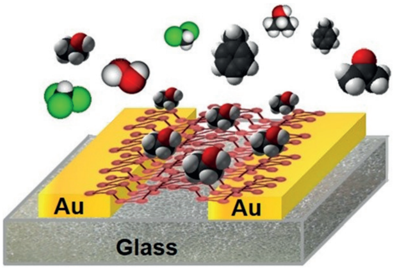

Vapor Sensors

C. C. Mayorga-Martinez, Z. Sofer, M. Pumera* ______ **14317 – 14320**

Layered Black Phosphorus as a Selective Vapor Sensor

Inside Back Cover

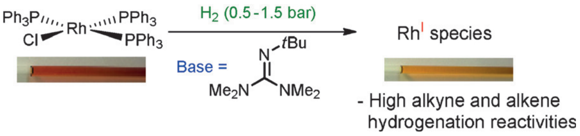

When Barton met Wilkinson: The simple addition of catalytic amounts of a strong Barton base to the well-known hydrogenation reaction promoted by Wilkinson's catalyst leads to a significant amplification of the reactivity. This reactivity is due to the formation of highly active rhodium(I) monohydride species.

Homogeneous Hydrogenation

J. E. Perea-Buceta, I. Fernández, S. Heikkinen, K. Axenov, A. W. T. King, T. Niemi, M. Nieger, M. Leskelä, T. Repo* ______ **14321 – 14325**

Diverting Hydrogenations with Wilkinson's Catalyst towards Highly Reactive Rhodium(I) Species

DNA Nanomachines

H. Zhang,* M. Lai, A. Zuehlke, H. Peng,
X.-F. Li, X. C. Le* ______ **14326 – 14330**

Binding-Induced DNA Nanomachines Triggered by Proteins and Nucleic Acids

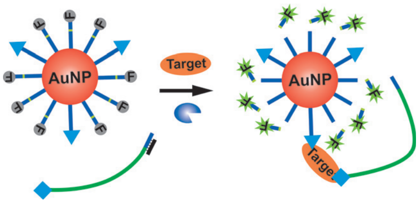

Binding of a target molecule to two ligands brings the swing arm to the gold nanoparticle (AuNP) and initiates autonomous, stepwise movement of the swing arm along the three-dimensional DNA tracks on the AuNP surface. The movement of the swing arm, powered by enzymatic cleavage of DNA anchorages, cleaves hundreds of oligonucleotides in response to a single binding event.

TiO_2 Electrodes

X. H. Gao, G. R. Li, Y. Y. Xu, Z. L. Hong,
C. D. Liang,* Z. Lin* ______ **14331 – 14335**

TiO_2 Microboxes with Controlled Internal Porosity for High-Performance Lithium Storage

TiO_2 microboxes demonstrate controlled internal porosity in the electrode for high-performance lithium ion batteries, which show superior lithium storage properties with a capacity of 187 mAh g^{-1} after 300 cycles at 1 C and good rate capabilities up to 20 C.

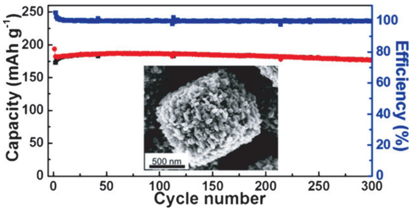

Peptide Folding

V. M. Kung, G. Cornilescu,
S. H. Gellman* ______ **14336 – 14339**

Impact of Strand Number on Parallel β-Sheet Stability

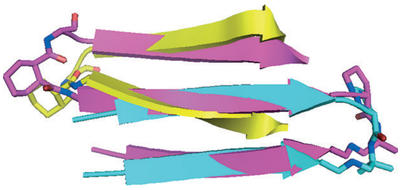

More strands, more stable: The first experimental model of a triple-stranded parallel β-sheet was designed. Analysis by NMR and circular dichroism spectroscopy offers the first experimental evidence that increasing the number of β-strands from two to three increases the stability of the parallel β-sheet.

Xenon Compounds

S. N. Britvin,* S. A. Kashtanov,
M. G. Krzhizhanovskaya, A. A. Gurinov,
O. V. Glumov, S. Strekopytov, Y. L. Kretser,
A. N. Zaitsev, N. V. Chukanov,
S. V. Krivovichev ______ **14340 – 14344**

Perovskites with the Framework-Forming Xenon

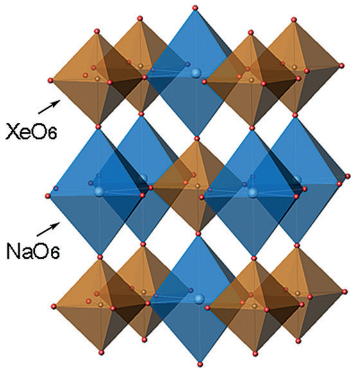

Xenon, the noble gas, can play the role of a framework-forming element in inorganic compounds, as is illustrated by the synthesis of a new family of double perovskites KM($XeNaO_6$) (M = Ca, Sr, Ba). The ability of xenon(VIII) to incorporate into stable inorganic frameworks might inspire new insights into the chemistry of this element as a crystal–chemical counterpart of group 4–5 transition metals: titanium, niobium, and tantalum.

Molecular Motors

L. Greb, A. Eichhöfer,
J.-M. Lehn* ______ **14345 – 14348**

Synthetic Molecular Motors: Thermal N Inversion and Directional Photoinduced C=N Bond Rotation of Camphorquinone Imines

Naturally simple: The thermal and photochemical *E*/*Z* isomerization of camphorquinone-derived imines was studied by a combination of kinetic, structural, and computational methods. Based on these studies of configurational switching in imine derivatives, chiral imines such as camphorquinone-based imines are proposed to be the simplest example of synthetic molecular motors.

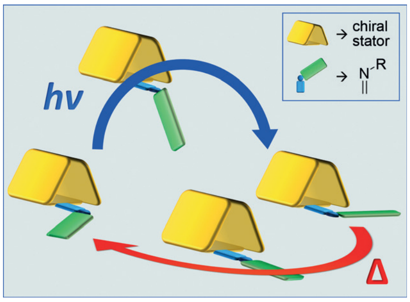

Metal–Organic Frameworks

E. Braun, J. J. Chen, S. K. Schnell, L.-C. Lin, J. A. Reimer,* B. Smit* ___ 14349 – 14352

Nanoporous Materials Can Tune the Critical Point of a Pure Substance

Vapor–liquid coexistence is suppressed in materials as the pore size approaches the order of the adsorbate molecule diameter. NMR relaxometry and molecular simulations show that such coexistence is possible in open metal–organic frameworks, and that the phases extend over many unit cells in a manner similar to bulk phase behaviour.

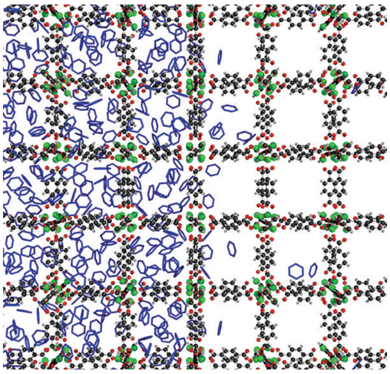

Paraffin Separation

A. H. Assen, Y. Belmabkhout, K. Adil, P. M. Bhatt, D.-X. Xue, H. Jiang, M. Eddaoudi* ___ 14353 – 14358

Ultra-Tuning of the Rare-Earth **fcu**-MOF Aperture Size for Selective Molecular Exclusion of Branched Paraffins

Back Cover

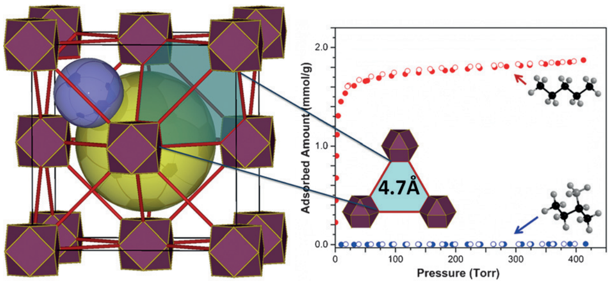

That's about the size of it: Isoreticular chemistry has permitted the deliberate design and construction of a new rare-earth (RE) **fcu**-MOF with suitable aperture size for the total separation of branched paraffins from normal paraffins.

Gas-Phase Chemistry

A. Troiani,* M. Rosi, S. Garzoli, C. Salvitti, G. de Petris* ___ 14359 – 14362

Iron-Promoted C—C Bond Formation in the Gas Phase

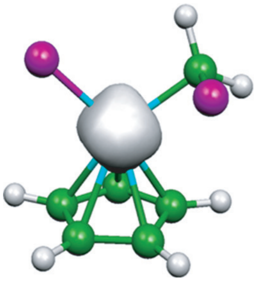

Ion–molecule reactions: A remarkable reorganization occured in iron-containing cations under ambient conditions. Fast and effective carbon–chlorine activation and carbon–carbon coupling was observed in gas-phase mixtures containing ferrocene and dichloromethane, through reaction intermediates (see picture) that eventually extrude the iron giving ferrous chloride.

Dual Catalysis

T. Sandmeier, S. Krautwald, H. F. Zipfel, E. M. Carreira* ___ 14363 – 14367

Stereodivergent Dual Catalytic α-Allylation of Protected α-Amino- and α-Hydroxyacetaldehydes

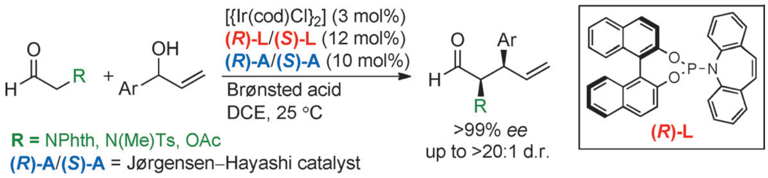

Be selective: Ir-catalyzed allylic substitution of racemic allylic alcohols with chiral enamines generated in situ enables the fully stereodivergent α-allylation of protected α-amino- and α-hydroxyacetaldehydes. The method furnishes α-N/O-substituted γ,δ-unsaturated aldehydes in good yields and with excellent enantioselectivities. Phth = phthalimide; cod = 1,5-cyclooctadiene; Ts = *p*-toluenesulfonyl; DCE = 1,2-dichloroethane.

Protein Labeling

Y. Hori, S. Hirayama, M. Sato,
K. Kikuchi* ________ 14368 – 14371

Redesign of a Fluorogenic Labeling System To Improve Surface Charge, Brightness, and Binding Kinetics for Imaging the Functional Localization of Bromodomains

Just a minute ... Rapid high-contrast imaging of intracellular proteins was made possible by a PYP-tag labeling system. By surface-charge engineering of the PYP-tag and the pK_a-based design of a fluorogenic probe, the labeling kinetics and brightness of the probe were significantly enhanced. The labeling system was used to detect the bromodomain–acetyl-histone interaction and its disruption by a bromodomain inhibitor.

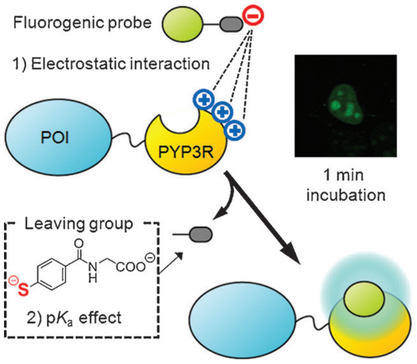

CO_2 Sorption

A. Kumar, D. G. Madden, M. Lusi,
K.-J. Chen, E. A. Daniels, T. Curtin,*
J. J. Perry IV,
M. J. Zaworotko* ________ 14372 – 14377

Direct Air Capture of CO_2 by Physisorbent Materials

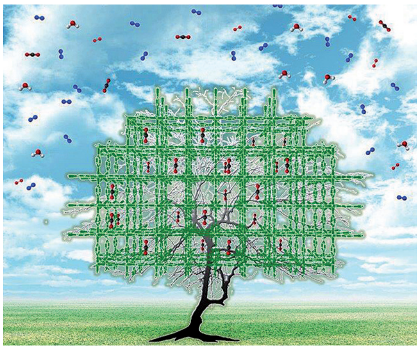

Five benchmark materials are investigated for their ability to adsorb CO_2 directly from air. It is found that physisorbents can compete with chemisorbents with respect to CO_2/N_2 selectivity but direct air capture (DAC) performance is mitigated because of competition with water vapor. Optimizing pore size and pore chemistry in the presence of water vapor must be further addressed if physisorbents are to compete with chemisorbents.

Metal–Organic Capsules

P. P. Neelakandan, A. Jiménez,
J. D. Thoburn,
J. R. Nitschke* ________ 14378 – 14382

An Autocatalytic System of Photooxidation-Driven Substitution Reactions on a $Fe^{II}_4L_6$ Cage Framework

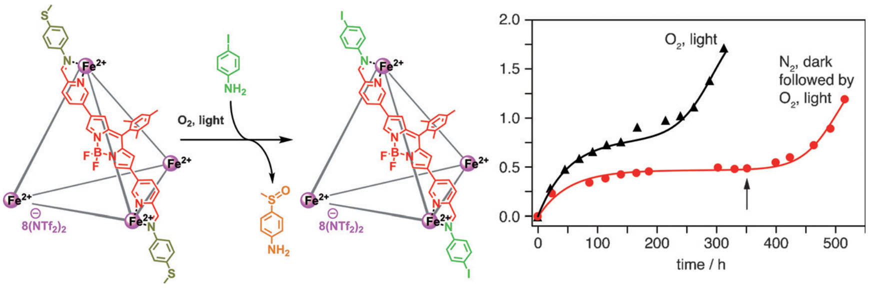

Sensitive operation: The incorporation of oxidizable (methylthio)aniline residues in $Fe^{II}_4L_6$ cages comprising $^1O_2$-sensitizing groups and dynamic-covalent imine bonds led to a system where photooxidation became autocatalytic: transformation of methylthio groups into sulfoxides renders the aniline residues electron-deficient enough for them to be displaced by iodoanilines, generating a better photocatalyst and accelerating the reaction.

Amyloid

C. A. De Carufel, N. Quittot, P. T. Nguyen,
S. Bourgault* ________ 14383 – 14387

Delineating the Role of Helical Intermediates in Natively Unfolded Polypeptide Amyloid Assembly and Cytotoxicity

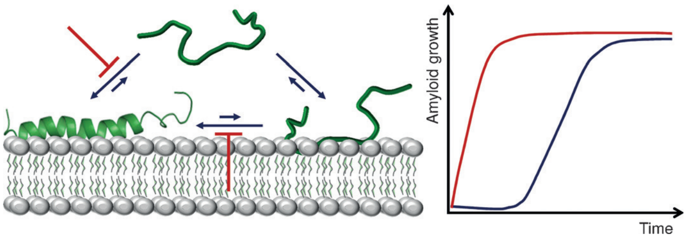

Amyloid formation resulting from the self-assembly of natively unfolded polypeptide was studied by means of a conformationally restricted derivative that co-assembles with the native peptide. Preventing islet amyloid polypeptide helical folding enhanced its amyloidogenicity in the presence of anionic biosurfaces and potentiated its toxicity towards pancreatic β-cells.

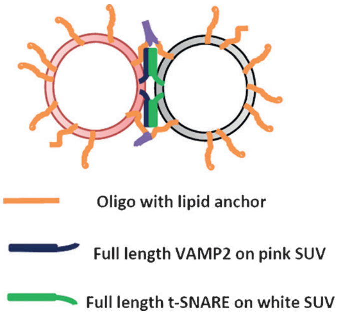

A non-fusogenic DNA–lipid mimic of tethering factors was developed that significantly stimulates SNARE-mediated lipid mixing. Using linkers with various lengths, two bridged membranes are kept within a controlled distance (see picture; SUV = small unilamellar vesicle). The DNA–lipid tethers can be applied to regulate other biological processes where capturing and bridging of two membranes are the prerequisites for protein function.

Vesicle Fusion

W. Xu, J. Wang, J. E. Rothman,*
F. Pincet* ———— **14388 – 14392**

Accelerating SNARE-Mediated Membrane Fusion by DNA–Lipid Tethers

---

Diastereomeric ratios up to > 98:2:0:0 can be obtained when stereodefined disubstituted silyl ketene aminals are used in Mukaiyama aldol reactions with aliphatic aldehydes to give highly selectively aldol products **1** with a quaternary carbon stereocenter α to the carbonyl group. The silyl ketene aminals are synthesized by a selective combined carbometalation–oxidation–silylation reaction.

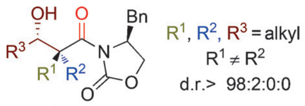

1

Asymmetric Synthesis

Z. Nairoukh, I. Marek* — **14393 – 14397**

Stereodefined Acyclic Polysubstituted Silyl Ketene Aminals: Asymmetric Formation of Aldol Products with Quaternary Carbon Stereocenters

---

Eu^{II} goes in vivo: Solid- and solution-phase characterization of the coordination environment of a europium(II)-containing cryptate are presented. This complex is employed in the measurement of the first in vivo images of contrast enhancement provided by a Eu^{II}-based contrast agent for magnetic resonance imaging.

Magnetic Resonance Imaging

L. A. Ekanger, L. A. Polin, Y. Shen,
E. M. Haacke, P. D. Martin,
M. J. Allen* ———— **14398 – 14401**

A Eu^{II}-Containing Cryptate as a Redox Sensor in Magnetic Resonance Imaging of Living Tissue

---

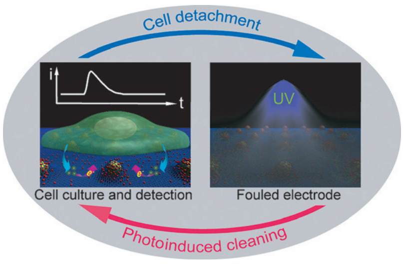

No electrode fouling: A versatile and efficient strategy based on photocatalytic cleaning is proposed for construction of a renewable electrochemical sensor used for cell analysis. The electrode was composed of TiO_2 nanoparticles wrapped by a reduced graphene oxide membrane and decorated by gold nanoparticles. The electrode was successfully used for biosensing at the single-cell level.

Biosensors

J.-Q. Xu, Y.-L. Liu, Q. Wang, H.-H. Duo,
X.-W. Zhang, Y.-T. Li,
W.-H. Huang* ———— **14402 – 14406**

Photocatalytically Renewable Micro-electrochemical Sensor for Real-Time Monitoring of Cells

Redox Chemistry

S. P. Heins, W. D. Morris,
P. T. Wolczanski,* E. B. Lobkovsky,
T. R. Cundari* ______ **14407 – 14411**

Nitrene Insertion into C–C and C–H Bonds of Diamide Diimine Ligands Ligated to Chromium and Iron

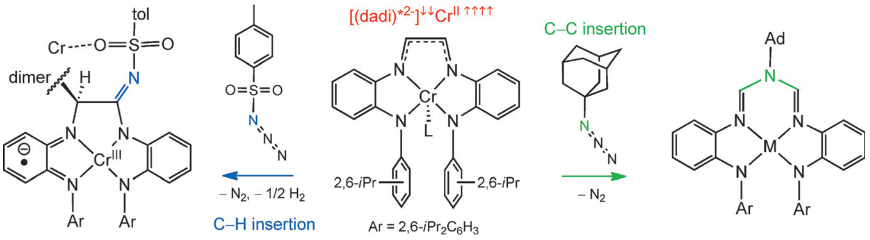

Who's your dadi? The implementation of a redox non-innocent diamide diimine (dadi)^n chelate enables intramolecular C–C and C–H nitrene insertion reactions. The reaction depends on the type of azide precursor used.

Hydrocarbons

X. Shi, W. Kueh, B. Zheng, K.-W. Huang,
C. Chi* ______ **14412 – 14416**

Dipolar Quinoidal Acene Analogues as Stable Isoelectronic Structures of Pentacene and Nonacene

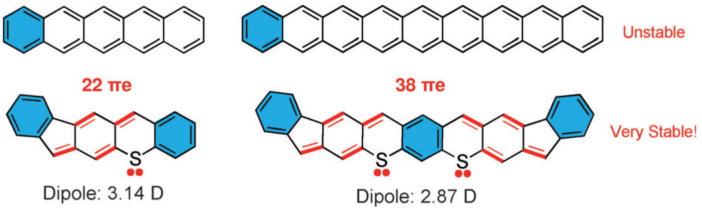

New arrivals on the "cene": Two dipolar quinoidal acene analogues were synthesized and they exhibit good solubility and high stability. They display distinctively different physical properties from the acene counterparts because of their closed-shell quinoidal structure with a dipolar character in the ground state. Unique packing structures were observed in single-crystal forms.

MOF Processing

C. Avci, J. Ariñez-Soriano,
A. Carné-Sánchez, V. Guillerm,
C. Carbonell, I. Imaz,*
D. Maspoch* ______ **14417 – 14421**

Post-Synthetic Anisotropic Wet-Chemical Etching of Colloidal Sodalite ZIF Crystals

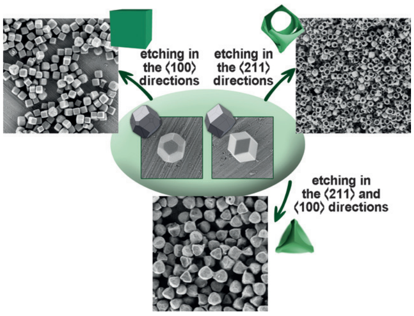

Post-synthetic wet-chemical anisotropic etching of colloidal ZIF-8 and ZIF-67 crystals enables uniform reshaping of them into unprecedented shapes, including cubic and tetrahedral crystals, and even hollow boxes, by an acid–base reaction and subsequent sequestration of leached metal ions.

Chirality

M. Parschau,
K.-H. Ernst* ______ **14422 – 14426**

Disappearing Enantiomorphs: Single Handedness in Racemate Crystals

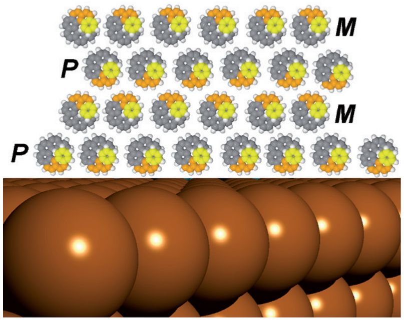

You'd better be on top! Racemic heptahelicene crystallizes into multilayered enantiomorphs in a homochiral-layer-by-homochiral-layer fashion on a Cu(111) surface (see picture). A small enantiomeric excess suppresses the formation of one enantiomorph and sends the minor enantiomer into the second layer, while the major enantiomer claims the bottom layer. Such enantiospecific dewetting of a metal surface is a new form of mirror-symmetry breaking.

Photocatalysis

J. Wang, T. V. Alves, F. J. Trindade,
C. B. de Aquino, J. C. Pieretti,
S. H. Domingues, R. A. Ando,
F. R. Ornellas,
P. H. C. Camargo* 14427 – 14431

Theoretical Design and Experimental Realization of Quasi Single Electron Enhancement in Plasmonic Catalysis

Add an extra electron! Under proper conditions, the static electric field induced by a single electron may become comparable to the electric-field intensities due to the surface plasmon resonance (SPR) excitation in plasmonic nanoparticles. By combining theoretical and experimental design, the effect of a quasi single electron on the near-field optical properties and SPR-mediated catalytic activities of Ag nanospheres was investigated.

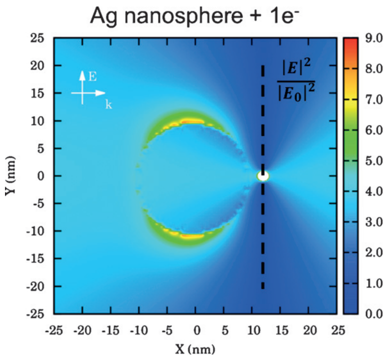

Glycosides

P. Shu, X. Xiao, Y. Zhao, Y. Xu, W. Yao,
J. Tao, H. Wang, G. Yao, Z. Lu, J. Zeng,
Q. Wan* 14432 – 14436

Interrupted Pummerer Reaction in Latent-Active Glycosylation: Glycosyl Donors with Recyclable and Regenerative Leaving Group

Actively latent: An efficient glycosylation enabled by an interrupted Pummerer reaction was successfully achieved. The active glycosyl donor possessing a recyclable and regenerative leaving group was obtained from a simple oxidation of the corresponding latent precursor. This strategy allowed the total synthesis and structural revision of the natural product leonoside F.

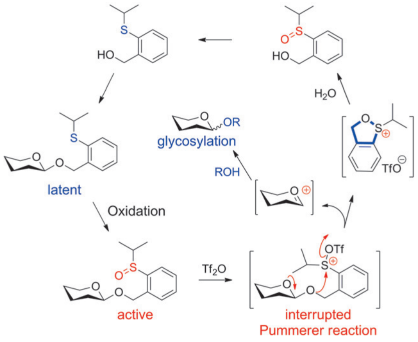

Nanocatalysis

T. Yurino, Y. Ueda, Y. Shimizu, S. Tanaka,
H. Nishiyama, H. Tsurugi, K. Sato,*
K. Mashima* 14437 – 14441

Salt-Free Reduction of Nonprecious Transition-Metal Compounds: Generation of Amorphous Ni Nanoparticles for Catalytic C–C Bond Formation

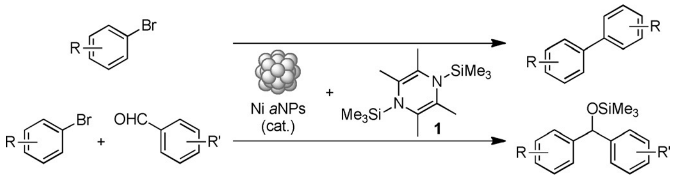

Small but mighty: Several nonprecious transition-metal compounds were reduced into the corresponding metallic particles under salt-free conditions using the organosilicon reductant **1**. Amorphous Ni nanoparticles (Ni *a*NPs) generated by this method from Ni(acac)$_2$ and **1** catalyzed reductive C–C bond formation reactions.

Chirality

F. Mamiya, N. Ousaka,*
E. Yashima* 14442 – 14446

Remote Control of the Planar Chirality in Peptide-Bound Metallomacrocycles and Dynamic-to-Static Planar Chirality Control Triggered by Solvent-Induced 3_{10}-to-α-Helix Transitions

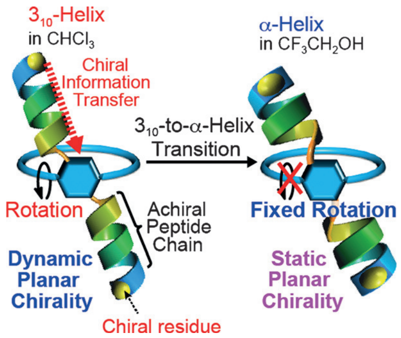

Locked rotation: The dynamic planar chirality in a nickel(II)-salphen-based macrocycle can be remotely controlled by a domino effect through the dynamic helical peptides that are bonded to the macrocycle rims. A solvent-induced conformational transition of the peptide chains from 3_{10}- to wider α-helices leads to kinetically trapped, static planar chirality.

Gold Catalysis

W. Zi, F. D. Toste* ______ 14447 – 14451

Gold(I)-Catalyzed Enantioselective Desymmetrization of 1,3-Diols through Intramolecular Hydroalkoxylation of Allenes

A chiral-anion-mediated enantioselective gold(I)-catalyzed desymmetrization of 1,3-diols by intramolecular allene hydroalkoxylation was developed. Subtle tuning of both the chiral phosphate (X*) and the achiral phosphine ligand (L) components of the catalyst system allowed for the preparation of oxygen heterocycles containing two stereocenters in high enantio- and diastereoselectivity.

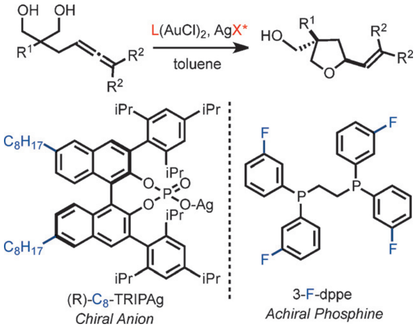

Heterocycle Synthesis

S. Huang, Y. Shao, L. Zhang, X. Zhou* ______ 14452 – 14456

Cycloamidination of Aminoalkenes with Nitriles: Synthesis of Substituted 2-Imidazolines and Tetrahydropyrimidines

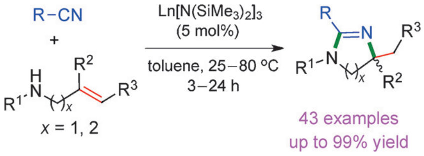

In rare form: The first catalytic cycloamidination of aminoalkenes and nitriles has been achieved by rare-earth complexes, and provides a straightforward and versatile method for atom-economical synthesis of substituted 2-imidazolines and tetrahydropyrimidines. The reaction features mild conditions, simple reagent and catalyst, high chemoselectivity, and 100% atom efficiency.

Natural Product Synthesis

T. Asaba, Y. Katoh, D. Urabe, M. Inoue* ______ 14457 – 14461

Total Synthesis of Crotophorbolone

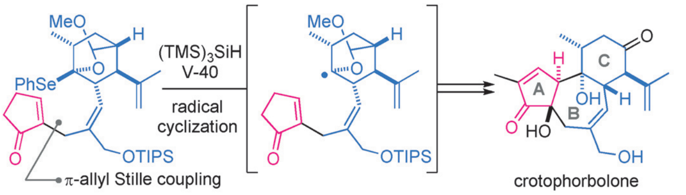

The complex ABC-tricyclic structure of crotophorbolone was assembled from (*R*)-carvone. After coupling of the six-membered C-ring and the five-membered A-ring through the π-allyl Stille coupling reaction, the α-alkoxy bridgehead radical reaction effected the *endo*-cyclization of the seven-membered B-ring by forming the sterically congested bond between the A- and C-rings. Functional-group manipulations resulted in the first total synthesis.

Controlled Polymerization

W. Xi, S. Pattanayak, C. Wang, B. Fairbanks, T. Gong, J. Wagner, C. J. Kloxin, C. N. Bowman* ______ 14462 – 14467

Clickable Nucleic Acids: Sequence-Controlled Periodic Copolymer/Oligomer Synthesis by Orthogonal Thiol-X Reactions

Click by click: The utilization of orthogonal thiol-X click reactions provides a method for sequence-controlled polymer synthesis. When combined with functional side groups in general and nucleobases in particular, this approach enables the formation of novel, highly functionalized materials in a robust, simple, and scalable manner (Trt = trityl).

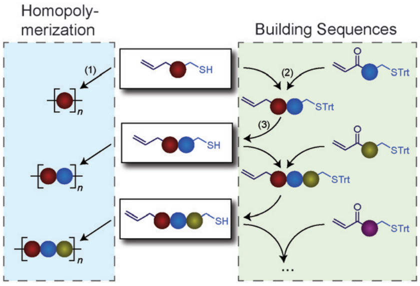

Front Cover

Charge Transfer

VIP

M. R. Talipov, T. S. Navale,
R. Rathore* ———— 14468 – 14472

The HOMO Nodal Arrangement in Polychromophoric Molecules and Assemblies Controls the Interchromophoric Electronic Coupling

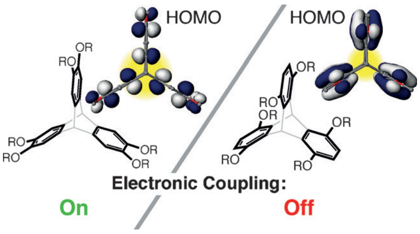

Pulling the plug: A visual inspection of the HOMOs enables the ready evaluation of the electronic coupling in cofacially arrayed polychromophoric molecules/assemblies. Both qualitative and quantitative applications of this simple approach can serve as powerful methods for the rational design of next-generation charge-transport materials for photovoltaic applications.

Artificial Ion Channels

Z. Sun, M. Barboiu,* Y.-M. Legrand,
E. Petit, A. Rotaru ———— 14473 – 14477

Highly Selective Artificial Cholesteryl Crown Ether K^+-Channels

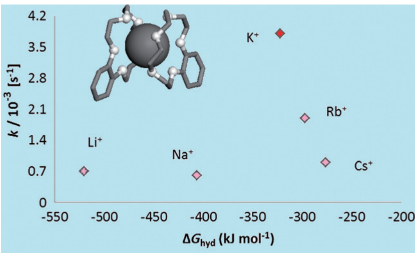

Crown ether ion channels: High selectivity for K^+ translocation through the artificial macrocycle channels is reminiscent of the conductance states of natural KcsA channels. It relates to the macrocycles binding ability surrounding the K^+ cations in a similar manner to the water molecules around the hydrated cation in water.

Platinum Anticancer Drugs

J. Kasparkova,* H. Kostrhunova,
O. Novakova, R. Křikavová, J. Vančo,
Z. Trávníček, V. Brabec ———— 14478 – 14482

A Photoactivatable Platinum(IV) Complex Targeting Genomic DNA and Histone Deacetylases

Two-in-one platinum anticancer drugs: The strategies based on simultaneous inhibition of histone deacetylases and DNA damage by platinum drugs induced by light may result in efficient antitumor activity taking advantages of selective and targeted activation in tumor cells.

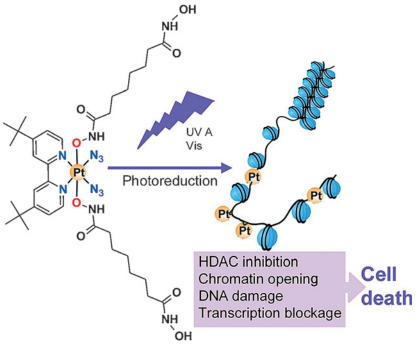

Green Chemistry

S. Elangovan, J.-B. Sortais,* M. Beller,
C. Darcel* ———— 14483 – 14486

Iron-Catalyzed α-Alkylation of Ketones with Alcohols

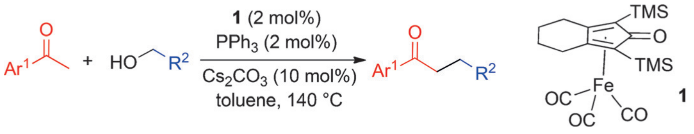

The α-alkylation reaction of ketones with primary alcohols leads in a straightforward and green manner to α-alkylated ketones using 2 mol% of an iron-based Knölker-type complex (**1**). Starting from 2-aminobenzylalcohol, the corresponding quinolone derivatives are obtained by the first iron-catalyzed Friedländer annulation reaction.

Hydrogen Borrowing

Z. W. Chen, H. Y. Zeng, S. A. Girard,
F. Wang, N. Chen,
C.-J. Li* ______ **14487 – 14491**

Formal Direct Cross-Coupling of Phenols with Amines

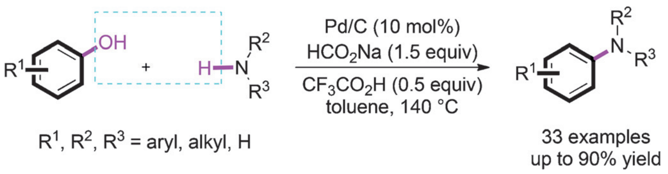

Give and take: The formal cross-coupling of phenols with various alkyl and aryl amines is catalyzed by Pd/C. A variety of substituted phenols were compatible with the reaction conditions, and secondary and tertiary aryl amines could thus be synthesized in moderate to excellent yields.

Luminogens

F. Bu, R. Duan, Y. Xie, Y. Yi, Q. Peng,*
R. Hu, A. Qin, Z. Zhao,*
B. Z. Tang* ______ **14492 – 14497**

Unusual Aggregation-Induced Emission of a Coumarin Derivative as a Result of the Restriction of an Intramolecular Twisting Motion

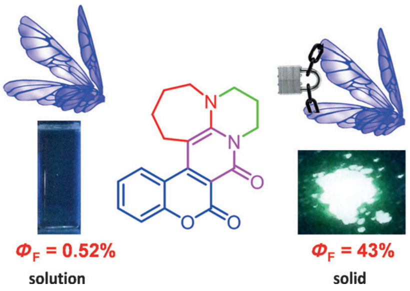

Let's twist again (in solution): The restriction of intramolecular twisting was shown experimentally and computationally to be the underlying mechanism for the aggregation-induced emission of a coumarin derivative. A large aliphatic ring promoted out-of-plane twisting of the molecular backbone in solution and thus nonradiative excited-state decay, whereas the restriction of this motion in aggregates led to strong fluorescence (see picture).

Low-Coordinate Complexes

C. M. Kelly, D.-H. Kwon, M. J. Ferguson,
S. M. Bischof, O. L. Sydora,* D. H. Ess,*
M. Stradiotto,*
L. Turculet* ______ **14498 – 14502**

Synthesis and Reactivity of a Neutral, Three-Coordinate Platinum(II) Complex Featuring Terminal Amido Ligation

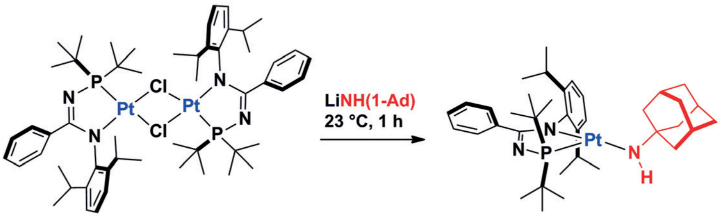

How low can you go? A formally 14 electron Pt^{II} complex featuring terminal amido ligation was isolated and characterized crystallographically (see scheme; 1-Ad = 1-adamantyl). A combination of stoichiometric reactivity studies and computational analysis confirmed the viability of net O–H and C–H addition across, as well as isonitrile insertion into, the terminal platinum–amido linkage of this unusual low-coordinate complex.

Carbenes

H. Luo, G. Wu, Y. Zhang,
J. Wang* ______ **14503 – 14507**

Silver(I)-Catalyzed *N*-Trifluoroethylation of Anilines and *O*-Trifluoroethylation of Amides with 2,2,2-Trifluorodiazoethane

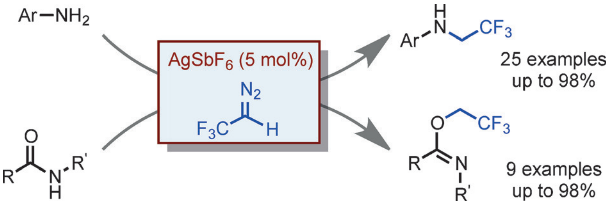

Insert carbene here: *N*-Trifluoroethylation of anilines has been developed through silver-catalyzed N–H insertions with CF_3CHN_2. The reaction is proposed to involve migratory insertion of a silver carbene as the key step. In contrast, *O*-trifluoroethylation occurs to afford trifluoroethyl imidates when amides are used as substrates under similar reaction conditions.

Reaction Mechanisms

V. Morozova, P. Mayer,
G. Berionni* ———— 14508 – 14512

Scope and Mechanisms of Frustrated Lewis Pair Catalyzed Hydrogenation Reactions of Electron-Deficient C=C Double Bonds

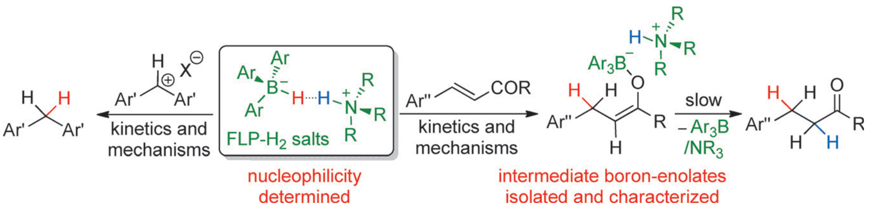

Nucleophilicity of FLPs: The nucleophilicity parameters of triarylborohydrides $Ar_3B^-H\cdots HN^+R_3$, intermediates in hydrogenation reactions catalyzed by frustrated Lewis pairs (FLPs; see scheme), were derived from reaction rates with various electrophiles. Investigations of the stepwise hydrogenation of electron-deficient C=C bonds with $Ar_3B^-H\cdots HN^+R_3$ revealed a strong effect of the substitution pattern in the Ar_3B catalyst on the hydride-donor reactivity.

Explosives

P. Yin, J. M. Shreeve* —— 14513 – 14517

From *N*-Nitro to *N*-Nitroamino: Preparation of High-Performance Energetic Materials by Introducing Nitrogen-Containing Ions

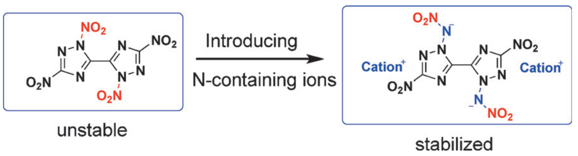

More N, more stable: The introduction of *N*-nitro and *N*-nitroamino functionalities in 1,2,4-triazoles was investigated. Comparative energetic measurements show that the *N*-nitroamino analogues, functionalized with additional nitrogen-rich anions and cations as energetic buffers, possess superior energetic performance and enhanced stability.

Heck Reaction

G. Meng, M. Szostak* —— 14518 – 14522

General Olefin Synthesis by the Palladium-Catalyzed Heck Reaction of Amides: Sterically Controlled Chemoselective N–C Activation

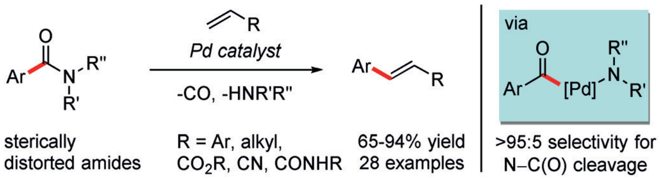

Welcome disturbance: The first Pd⁰-catalyzed Heck reaction of amides proceeding through highly chemoselective N–C activation utilizing amide bond ground-state distortion is reported. The reaction shows excellent functional group tolerance and avoids the formation of corrosive halide waste (base-free Heck). It provides access to a myriad of metal-catalyzed transformations of amides through metal insertion/decarbonylation.

Silanes

I. Buslov, J. Becouse, S. Mazza,
M. Montandon-Clerc,
X. Hu* ———— 14523 – 14526

Chemoselective Alkene Hydrosilylation Catalyzed by Nickel Pincer Complexes

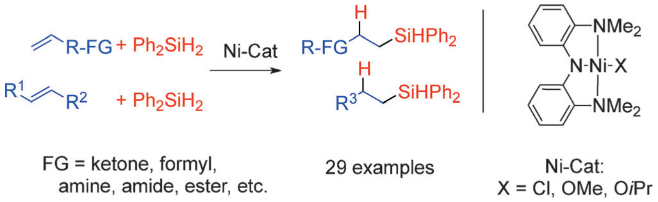

High turnover: Well-defined bis(amino)amide nickel pincer complexes are efficient catalysts for anti-Markovnikov hydrosilylation of terminal alkenes. The turnover frequencies are up to 83 000 per hour and turnover numbers are up to 10 000. The C=C bonds of alkenes containing amino, ester, amido, ketone, and formyl groups are selectively hydrosilylated.

NMR Spectroscopy

N. Eshuis, R. L. E. G. Aspers,
B. J. A. van Weerdenburg, M. C. Feiters,
F. P. J. T. Rutjes, S. S. Wijmenga,
M. Tessari* ______ **14527 – 14530**

2D NMR Trace Analysis by Continuous Hyperpolarization at High Magnetic Field

NMR trace analysis: Continuous hyperpolarization at high magnetic field is employed for the investigation of dilute analytes through their two-dimensional NMR correlations with para-H_2-derived hydrides (see picture). The combination of 2D NMR resonance dispersion and para-H_2-induced signal enhancement allows detection and quantification of nanomolar concentrations in complex mixtures.

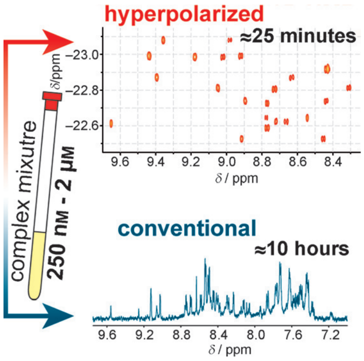

Vaccine Scaffolds

X. Luo, T. Liu, Y. Wang, H. Jia, Y. Zhang,
D. Caballero, J. Du, R. E. Wang, D. Wang,
P. G. Schultz,* F. Wang* **14531 – 14534**

An Epitope-Specific Respiratory Syncytial Virus Vaccine Based on an Antibody Scaffold

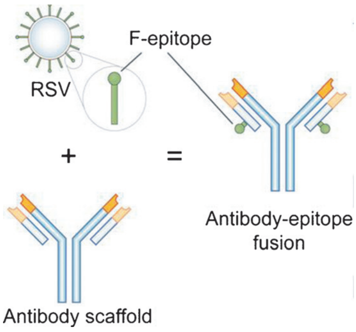

Vaccine scaffolds based on antibody-epitope fusions: Fusion of a virus-neutralizing epitope (green) into the complementarity-determining region (CDR) or constant loops of an immunoglobulin provides a strategy for generating epitope-focused vaccines.

Fluoroalkyl Ammonium Salts

A. F. Baxter, K. O. Christe,
R. Haiges* ______ **14535 – 14538**

Convenient Access to α-Fluorinated Alkylammonium Salts

Effing and binding: HF addition across the C≡N triple bonds of various nitriles and subsequent addition of MF_5 (M = As, Sb) yields room-temperature stable α-fluoroalkyl ammonium salts. The cations $[HCF_2NH_3]^+$, $[CF_3NH_3]^+$, $[CF_3CF_2NH_3]^+$, $[HCF_2CF_2NH_3]^+$, and $[(NH_3CF_2)_2]^{2+}$ were prepared and isolated as $[AsF_6]^-$, $[SbF_6]^-$, and $[Sb_2F_{11}]^-$ salts.

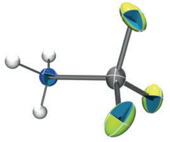
$[CF_3NH_3]^+$

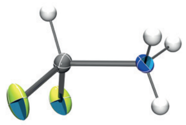
$[HCF_2NH_3]^+$

Nanoparticle Synthesis

Z. Fan, X. Chen, M. Köhn Serrano,
H. Schmalz, S. Rosenfeldt, S. Förster,
S. Agarwal, A. Greiner* __ **14539 – 14544**

Polymer Cages as Universal Tools for the Precise Bottom-Up Synthesis of Metal Nanoparticles

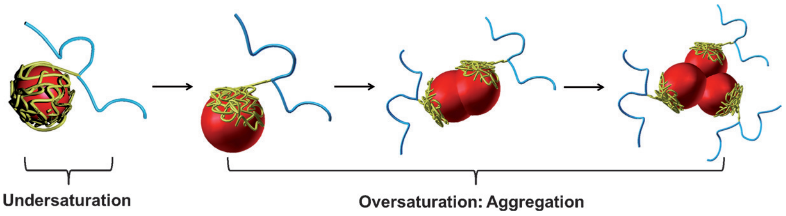

Being cagey: Polymer cages with sulfur moieties prepared by the “grafting-around” method were used as templates for the precise and size-controlled bottom-up synthesis of metal nanoparticles. In contrast to the use of block copolymers as ligands for nanoparticles, the polymer cages exhibited the capacity for controlled nanoparticle encapsulation, which enabled their use as ideal templates for nanoparticles.

Light-induced formation of coumarin from *o*-hydroxycinnamates was used to establish a new strategy for manipulating the solubility of polymers. The corresponding spin-coated films display complete insolubility in organic solvents and a drastic increase in performance as the emitting layer of OLEDs after irradiation.

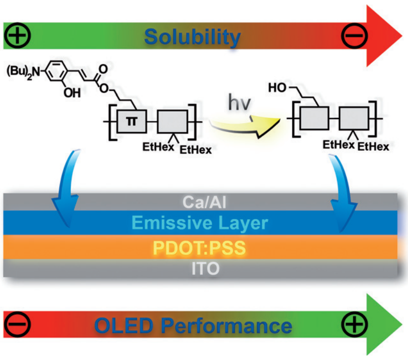

OLEDs

K. M. Schelkle, M. Bender, K. Jeltsch,
T. Buckup, K. Müllen, M. Hamburger,
U. H. F. Bunz* **14545–14548**

Light-Induced Solubility Modulation of Polyfluorene To Enhance the Performance of OLEDs

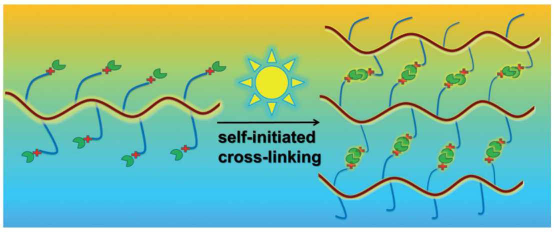

Photoactive polymer-based nanoparticles and porous materials were formed by the side-product- and surfactant-free self-initiated cross-linking of a conjugated polymer bearing vinylimidazolium side groups. The polymer acts as both a photosensitizer and a stabilizer for colloidal systems. The obtained cross-linked polymers serve as efficient, recyclable, cost-effective heterogeneous photocatalysts under visible-light irradiation.

Photocatalysts

S. Ghasimi, S. Prescher, Z. J. Wang,
K. Landfester, J. Yuan,*
K. A. I. Zhang* **14549–14553**

Heterophase Photocatalysts from Water-Soluble Conjugated Polyelectrolytes: An Example of Self-Initiation under Visible Light

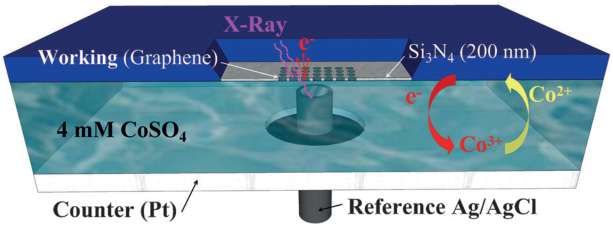

The electronic structure of cobalt on graphene was investigated with a new flow cell that provides electronic and chemical information on the active surfaces by means of X-ray photoelectron spectroscopy. It is shown that cobalt is anchored on graphene via carbonyl-like species, promoting the reduction of Co^{3+} to Co^{2+}, which is believed to be the active site of the catalyst.

Electrocatalysis

J. J. Velasco-Velez,* V. Pfeifer,
M. Hävecker, R. S. Weatherup, R. Arrigo,
C.-H. Chuang, E. Stotz, G. Weinberg,
M. Salmeron, R. Schlögl,
A. Knop-Gericke **14554–14558**

Photoelectron Spectroscopy at the Graphene–Liquid Interface Reveals the Electronic Structure of an Electrodeposited Cobalt/Graphene Electrocatalyst

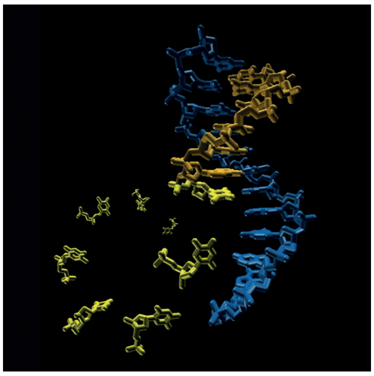

Copying of RNA without a chemist: Ribonucleotides are incorporated efficiently at the terminus of a growing RNA strand in enzyme-free, template-directed fashion under "general condensation conditions".

RNA Chemistry

M. Jauker, H. Griesser,
C. Richert* **14559–14563**

Copying of RNA Sequences without Pre-Activation

RNA Chemistry

M. Jauker, H. Griesser,
C. Richert* ______ **14564 – 14569**

Spontaneous Formation of RNA Strands, Peptidyl RNA, and Cofactors

The peptidyl RNA world: RNA strands, peptidyl RNAs, and cofactors emerge spontaneously, without chemical pre-activation, when solutions of building blocks are exposed to condensation conditions.

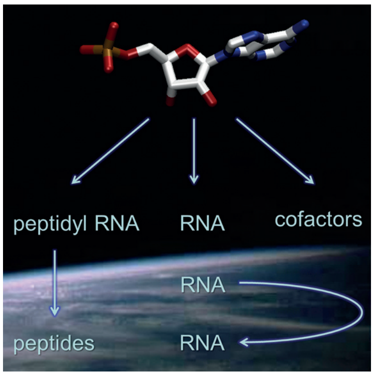

Molecular Machines

A.-M. Stadler,* L. Karmazin,
C. Bailly ______ **14570 – 14574**

A Ca^{2+}-, Mg^{2+}-, and Zn^{2+}-Based Dendritic Contractile Nanodevice with Two pH-Dependent Motional Functions

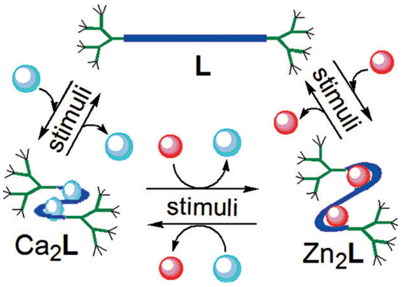

Contract and stretch: A dendrimer has been developed that contracts upon metal-ion coordination (Ca^{2+}, Mg^{2+}, Zn^{2+}) and changes its height upon transmetalation (displacement of Ca^{2+} by Zn^{2+}). These nanomechanical motions were made pH-dependent.

Drug Design

W. Jahnke,* G. Bold, A. L. Marzinzik,
S. Ofner, X. Pellé, S. Cotesta, E. Bourgier,
S. Lehmann, C. Henry, R. Hemmig,
F. Stauffer, J. C. D. Hartwieg, J. R. Green,
J.-M. Rondeau ______ **14575 – 14579**

A General Strategy for Targeting Drugs to Bone

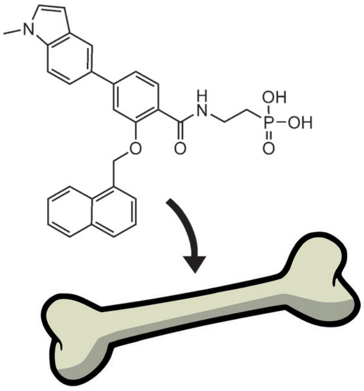

To the bone: Drugs for bone diseases benefit from targeting to bone. Bone-affinity tags are presented that can be attached to bone-acting drug molecules to make them safer and more efficacious, while retaining desired properties such as cellular permeability and oral bioavailability. This was demonstrated for allosteric inhibitors of farnesyl pyrophosphate synthase.

Transport Processes

T. Titze, A. Lauerer, L. Heinke, C. Chmelik,
N. E. R. Zimmermann, F. J. Keil,
D. M. Ruthven, J. Kärger* **14580 – 14583**

Transport in Nanoporous Materials Including MOFs: The Applicability of Fick's Laws

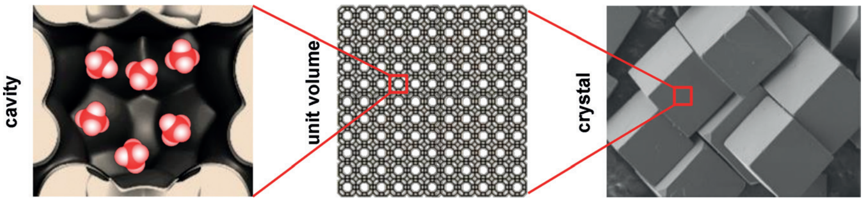

No more diffusion confusion: Although the elementary steps of molecular propagation in nanoporous materials may be quite intricate, overall mass transfer in the individual particles generally follows the simple Fickian laws of diffusion. Even in a complex system, the diffusion coefficient is a well-defined quantity and the addition of qualifiers such as "effective", "seeming", or "apparent" is unnecessary and even misleading.

Supporting information is available on www.angewandte.org (see article for access details).

A video clip is available as Supporting Information on www.angewandte.org (see article for access details).

This article is available online free of charge (Open Access).

This article is accompanied by a cover picture (front or back cover, and inside or outside).

The Very Important Papers, marked VIP, have been rated unanimously as very important by the referees.

The Hot Papers are articles that the Editors have chosen on the basis of the referee reports to be of particular importance for an intensely studied area of research.

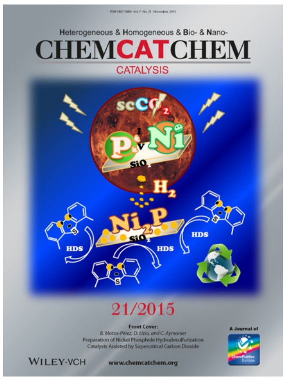

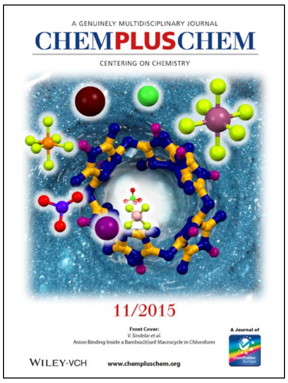

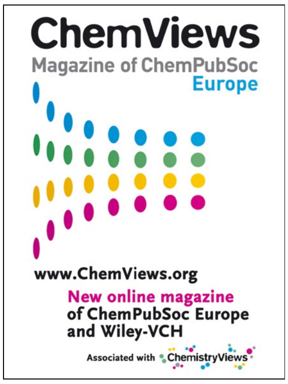

Angewandte Corrigendum

Compounds **12** and **21** are drawn correctly in the Supporting Information along with their spectral characterizations (Figure S4l and Figure S4u). However, those compounds were depicted incorrectly in Scheme 2 of this Communication. The proper entries in Scheme 2 are shown below.

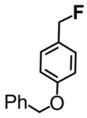

12, 58%[d]

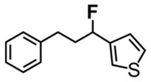

21, 56%[c]

Targeted Fluorination with the Fluoride Ion by Manganese-Catalyzed Decarboxylation

X. Huang, W. Liu, J. M. Hooker, J. T. Groves* ———— **5241–5245**

Angew. Chem. Int. Ed. **2015**, *54*

DOI: 10.1002/anie.201500399

Angewandte Addendum

In this Communication, a reference to a pertinent prior investigation is missing. The work by Thomas and co-workers should be cited as Ref. [40] on page 12734, left column, first line after "… and different alkyne monomers were successfully produced by a Sonogashira–Hagihara coupling reaction.[40]"

---

[40] S. Fischer, J. Schmidt, P. Strauch, A. Thomas, *Angew. Chem. Int. Ed.* **2013**, *52*, 12174 – 12178; *Angew. Chem.* **2013**, *125*, 12396 – 12400.

Highly Efficient Enrichment of Volatile Iodine by Charged Porous Aromatic Frameworks with Three Sorption Sites

Z. Yan, Y. Yuan, Y. Tian, D. Zhang, G. Zhu* ———— **12733–12737**

Angew. Chem. Int. Ed. **2015**, *54*

DOI: 10.1002/anie.201503362

Angewandte Retraction

Direct Allylation of In Situ Generated Aldehyde Acyl Anions by Synergistic NHC and Palladium Catalysis

M. M. Ahire, S. B. Mhaske* **7038–7042**

Angew. Chem. Int. Ed. **2014**, *53*

DOI: 10.1002/anie.201400623

The above article from *Angewandte Chemie International Edition*, published online on May 21, 2014 in Wiley Online Library (www.onlinelibrary.wiley.com, DOI: 10.1002/anie.201400623) and in print,[1] has been retracted by agreement between the corresponding author, the journal Editor, Dr. Peter Gölitz, and Wiley-VCH Verlag GmbH & Co. KGaA, Weinheim. The retraction has been agreed upon because by performing additional characterization data analyses, the authors discovered that the structures of the products (table 1) were incorrectly assigned: A double-check of the data revealed that the major isolated products were allyl esters and not the expected allyl ketones. The authors acknowledge this severe mistake and its potential impact on the community.

---

[1] M. M. Ahire, S. B. Mhaske, *Angew. Chem. Int. Ed.* **2014**, *53*, 7038 – 7042; *Angew. Chem.* **2014**, *126*, 7158 – 7162; corrigendum: M. M. Ahire, S. B. Mhaske, *Angew. Chem. Int. Ed.* **2015**, *54*, 8321; *Angew. Chem.* **2015**, *127*, 8439.